

The flavor asymmetry of polarized anti-quarks in the nucleon

F.-G. Cao^a, A.I. Signal^b

Institute of Fundamental Sciences, Massey University, Private Bag 11 222, Palmerston North, New Zealand

Received: 12 April 2001 / Revised version: 30 May 2001 /

Published online: 19 July 2001 – © Springer-Verlag / Società Italiana di Fisica 2001

Abstract. We present a study of the flavor asymmetry of polarized anti-quarks in the nucleon using the meson cloud model. We include contributions both from the vector mesons and the interference terms of pseudoscalar and vector mesons. Employing the bag model, we first give the polarized valence quark distribution of the ρ meson and the interference distributions. Our calculations show that the interference effect mildly increases the prediction for $\Delta\bar{d}(x) - \Delta\bar{u}(x)$ at intermediate x region. We also discuss the contribution of “Pauli blocking” to the asymmetry.

1 Introduction

The possible breaking of parton model symmetries by the nucleon’s quark distribution functions has been a topic of great interest since the experimental discoveries that the Ellis–Jaffe [1] and Gottfried [2] sum rules are violated. In particular, the flavor asymmetry in the nucleon sea ($\bar{d} > \bar{u}$) has been confirmed by several experiments [3, 4], and the x -dependence of this asymmetry has been investigated. This asymmetry can be naturally explained in the meson cloud model, in which the physical nucleon wave function contains many virtual meson–baryon components, and the valence anti-quark in the meson contributes (via a convolution) to the anti-quark distributions in the proton sea. Since the probability of the Fock state $|n\pi^+\rangle$ is larger than that of the $|\Delta^{++}\pi^-\rangle$ state in the proton wave function, the asymmetry $\bar{d} > \bar{u}$ emerges naturally in the proton sea. There have been many theoretical investigations (see e.g. [5–8] and references therein) on this subject.

Recently, there has been increasing interest in the question of whether this asymmetry extends also to the polarized sea distributions, i.e. $\Delta\bar{d}(x) \neq \Delta\bar{u}(x)$. Such a polarized sea asymmetry would make a direct contribution to the Bjorken sum rule. Although well established experimental evidence for a polarized sea asymmetry is still lacking, some experimental studies have been done [9]. Moreover, several parameterizations [10] for the polarized parton distributions arising from fits of the world data from polarized experiments leave open the possibility of this asymmetry. There have also been some theoretical studies on this asymmetry. In [11, 12], the polarized sea asymmetries are calculated in the chiral quark-soliton model (us-

ing the large- N_C limit). Sizable results for $\Delta\bar{d}(x) - \Delta\bar{u}(x)$ and $\Delta\bar{d}(x) + \Delta\bar{u}(x) - 2\Delta\bar{s}(x)$ were found, and it was further predicted that the flavor asymmetry of the polarized sea distributions is larger than that of the unpolarized sea distributions, i.e. $|\Delta\bar{d}(x) - \Delta\bar{u}(x)| > |\bar{d}(x) - \bar{u}(x)|$. Such sizable asymmetries would make an important contribution (around 20%) to the Bjorken sum rule. Fries and Schäfer [13] calculated the non-strange polarized sea asymmetry by considering the ρ meson cloud in the meson cloud model. Their prediction for $\Delta\bar{d}(x) - \Delta\bar{u}(x)$ is more than one order of magnitude smaller than the result from the chiral quark-soliton model. Boreskov and Kaidalov [14] analyzed this asymmetry by calculating the Regge cut contribution to the imaginary part of the high-energy photon–nucleon scattering amplitude. They found that the interference between the amplitudes for the photon coupling to a pion or to a rho meson can provide a sizable polarized anti-quark asymmetry in the small x region. This asymmetry has also been discussed in the instanton model [15] and a statistical model [16] for the parton distributions of the nucleon.

In this paper we investigate the flavor asymmetry of the non-strange polarized anti-quarks using the meson cloud model. We include both the vector meson cloud and the interference terms of the pseudoscalar and the vector mesons. Such interference terms appear naturally in the meson cloud model.

In Sect. 2, we derive the formulas in the meson cloud model to calculate the flavor asymmetry of non-strange polarized anti-quark distributions. The numerical results are given in Sect. 3 along with a discussion. In Sect. 4, we discuss how a contribution to the flavor asymmetry can arise from the fermion nature of the quarks, often called Pauli blocking. Section 5 is a summary.

^a e-mail: f.g.cao@massey.ac.nz

^b e-mail: a.i.signal@massey.ac.nz

2 Flavor asymmetry in the meson cloud model

In the meson cloud model (MCM) the nucleon can be viewed as a bare nucleon plus some meson–baryon Fock states which result from the fluctuation $N \rightarrow MB$. The wave function of the nucleon can be written as [6]

$$|N\rangle_{\text{physical}} = Z|N\rangle_{\text{bare}} + \sum_{MB} \sum_{\lambda\lambda'} \int dy d^2\mathbf{k}_\perp \phi_{MB}^{\lambda\lambda'}(y, k_\perp^2) \times |M^\lambda(y, \mathbf{k}_\perp); B^{\lambda'}(1-y, -\mathbf{k}_\perp)\rangle, \quad (1)$$

where Z is the wave function renormalization constant, $\phi_{MB}^{\lambda\lambda'}(y, k_\perp^2)$ is the wave function of the Fock state containing a meson (M) with longitudinal momentum fraction y , transverse momentum \mathbf{k}_\perp , and helicity λ , and a baryon (B) with momentum fraction $1-y$, transverse momentum $-\mathbf{k}_\perp$, and helicity λ' . The model assumes that the life time of a virtual baryon–meson Fock state is much larger than the interaction time in the deep inelastic or Drell–Yan process, thus the quark and anti-quark in the virtual meson–baryon Fock states can contribute to the parton distributions of the nucleon. For spin independent parton distributions these non-perturbative contribution can usually be expressed as a convolution of fluctuation functions with the valence parton distributions in the meson and/or baryon. For polarized parton distributions in the model it is necessary to include all the terms which can lead to the same final state [17]. This allows for the possibility of interference terms between different terms in the nucleon wave function (1). The effect of interference between $N\pi$ and $\Delta\pi$ terms on polarized quark distributions was calculated in [18,19]. For polarized anti-quark distributions the interference will be between terms with different mesons and the same baryon, e.g. $N\pi$ and $N\rho$; see Fig. 1.

We can write the total meson cloud contribution to the distribution of anti-quarks of a given flavor with helicity σ as

$$x\delta\bar{q}^\sigma(x) = \sum_\lambda \int_x^1 dy f_{(M_1 M_2)B/N}^\lambda(y) \times \frac{x}{y} \bar{q}_{(M_1 M_2)\lambda}^\sigma\left(\frac{x}{y}\right), \quad (2)$$

where

$$f_{(M_1 M_2)B/N}^\lambda(y) = \sum_{\lambda'} \int_0^\infty dk_\perp^2 \phi_{M_1 B}^{\lambda\lambda'}(y, k_\perp^2) \phi_{M_2 B}^{*\lambda\lambda'}(y, k_\perp^2) \quad (3)$$

is the helicity dependent fluctuation function. The second meson (M_2) could be the same as or different from the first meson (M_1).

For simplicity we denote (2) as

$$x\delta\bar{q}^\sigma = \sum_\lambda f_{(M_1 M_2)B/N}^\lambda \otimes \bar{q}_{(M_1 M_2)\lambda}^\sigma. \quad (4)$$

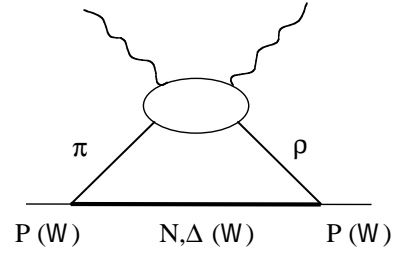


Fig. 1. Schematic illustration of interference contributions to the polarized anti-quark distributions

The two mesons appearing in (4) may be both vector mesons (V) or one pseudoscalar meson (P) plus one vector meson (V), that is

$$x\delta\bar{q}^\sigma = \sum_{\lambda=0,\pm 1} f_{VB/N}^\lambda \otimes \bar{q}_{V\lambda}^\sigma + \sum_{\lambda=0,\pm 1} f_{(V_1 V_2)B/N}^\lambda \otimes \bar{q}_{(V_1 V_2)\lambda}^\sigma + \sum_{\lambda=0} f_{(PV)B/N}^0 \otimes \bar{q}_{(PV)_0}^\sigma. \quad (5)$$

Observing that (see the discussion below)

$$\bar{q}_{(V_1 V_2)_1}^\uparrow = \bar{q}_{(V_1 V_2)_{-1}}^\downarrow, \quad \bar{q}_{(V_1 V_2)_1}^\downarrow = \bar{q}_{(V_1 V_2)_{-1}}^\uparrow, \\ \bar{q}_{(V_1 V_2)_0}^\uparrow = \bar{q}_{(V_1 V_2)_0}^\downarrow, \quad \bar{q}_{(PV)_0}^\uparrow \neq \bar{q}_{(PV)_0}^\downarrow, \quad (6)$$

and denoting

$$\Delta f_{(V_1 V_2)B/N} = f_{(V_1 V_2)B/N}^1 - f_{(V_1 V_2)B/N}^{-1}, \quad (7)$$

$$\Delta \bar{q}_{V_1 V_2} = \bar{q}_{(V_1 V_2)_1}^\uparrow - \bar{q}_{(V_1 V_2)_{-1}}^\downarrow, \\ \Delta \bar{q}_{(PV)_0} = \bar{q}_{(PV)_0}^\uparrow - \bar{q}_{(PV)_0}^\downarrow, \quad (8)$$

we have

$$x(\Delta\bar{q}) = x\delta\bar{q}^\uparrow - x\delta\bar{q}^\downarrow \\ = \Delta f_{VB/N} \otimes \Delta\bar{q}_V + \Delta f_{(V_1 V_2)B/N} \otimes \Delta\bar{q}_{V_1 V_2} \\ + f_{(PV)B/N} \otimes \Delta\bar{q}_{PV}. \quad (9)$$

The first term in (9) comes from the vector meson cloud, which has been considered in [13]. The second and third terms, which are first included in this study, result from the interference between terms with two different vector mesons (ρ, ω) and between terms with a vector meson (ρ, ω) and a pseudoscalar meson (π) respectively. Equation (9) explicitly shows the existence of the interference contributions. We would like to point out that the above interference terms do not contribute to the unpolarized parton distributions due to the flavor–spin structure of the $SU(6)$ wave function. For example, the $\pi^+-\rho^+$ interference term contributes to \bar{d}^\uparrow and \bar{d}^\downarrow with equal magnitude but opposite sign (see the below expressions for the wave functions), so the result is zero when the helicities are summed. The $SU(6)$ wave function also leads to a zero contribution to the polarized anti-quark distribution from $\pi-\eta$ interference terms.

The interference distributions ($\Delta\bar{q}_{\rho\omega}, \Delta\bar{q}_{\pi\rho}, \Delta\bar{q}_{\pi\omega}, q = u, d$) do not have the same straightforward interpretation as the quark distributions. However, using the quark

model with $SU(6)$ wave functions we can relate these distributions to the polarized anti-quark distributions of the vector mesons. In the quark model, the valence wave functions of the π , ρ and ω mesons can be written as [20]

$$\begin{aligned} |\pi^+\rangle &= \frac{1}{\sqrt{2}}(\bar{d}^\uparrow u^\downarrow - \bar{d}^\downarrow u^\uparrow)\psi_\pi(x, k_\perp), \\ |\pi^0\rangle &= \frac{1}{2}(\bar{u}^\uparrow u^\downarrow - \bar{u}^\downarrow u^\uparrow - \bar{d}^\uparrow d^\downarrow + \bar{d}^\downarrow d^\uparrow)\psi_\pi(x, k_\perp), \\ |\pi^-\rangle &= \frac{1}{\sqrt{2}}(\bar{u}^\uparrow d^\downarrow - \bar{u}^\downarrow d^\uparrow)\psi_\pi(x, k_\perp), \end{aligned} \quad (10)$$

$$\begin{aligned} |\rho^+\rangle^{1,1} &= \bar{d}^\uparrow u^\uparrow\psi_\rho(x, k_\perp), \\ |\rho^+\rangle^{1,0} &= \frac{1}{\sqrt{2}}(\bar{d}^\uparrow u^\downarrow + \bar{d}^\downarrow u^\uparrow)\psi_\rho(x, k_\perp), \\ |\rho^+\rangle^{1,-1} &= \bar{d}^\downarrow u^\downarrow\psi_\rho(x, k_\perp), \\ |\rho^0\rangle^{1,1} &= \frac{1}{\sqrt{2}}(\bar{u}^\uparrow u^\uparrow - \bar{d}^\uparrow d^\uparrow)\psi_\rho(x, k_\perp), \\ |\rho^0\rangle^{1,0} &= \frac{1}{2}(\bar{u}^\uparrow u^\downarrow + \bar{u}^\downarrow u^\uparrow - \bar{d}^\uparrow d^\downarrow - \bar{d}^\downarrow d^\uparrow)\psi_\rho(x, k_\perp), \\ |\rho^0\rangle^{1,-1} &= \frac{1}{\sqrt{2}}(\bar{u}^\downarrow u^\downarrow - \bar{d}^\downarrow d^\downarrow)\psi_\rho(x, k_\perp), \\ |\rho^-\rangle^{1,1} &= \bar{u}^\uparrow d^\uparrow\psi_\rho(x, k_\perp), \\ |\rho^-\rangle^{1,0} &= \frac{1}{\sqrt{2}}(\bar{u}^\uparrow d^\downarrow + \bar{u}^\downarrow d^\uparrow)\psi_\rho(x, k_\perp), \\ |\rho^-\rangle^{1,-1} &= \bar{u}^\downarrow d^\downarrow\psi_\rho(x, k_\perp), \end{aligned} \quad (11)$$

$$\begin{aligned} |\omega\rangle^{1,1} &= \frac{1}{\sqrt{2}}(\bar{u}^\uparrow u^\uparrow + \bar{d}^\uparrow d^\uparrow)\psi_\omega(x, k_\perp), \\ |\omega\rangle^{1,0} &= \frac{1}{2}(\bar{u}^\uparrow u^\downarrow + \bar{u}^\downarrow u^\uparrow + \bar{d}^\uparrow d^\downarrow + \bar{d}^\downarrow d^\uparrow)\psi_\omega(x, k_\perp), \\ |\omega\rangle^{1,-1} &= \frac{1}{\sqrt{2}}(\bar{u}^\downarrow u^\downarrow + \bar{d}^\downarrow d^\downarrow)\psi_\omega(x, k_\perp), \end{aligned} \quad (12)$$

where $\psi_M(x, k_\perp)$ is a two-body light-cone wave function. The ω meson has been treated as an ideal mixture of an octet and a singlet. Note that the distribution $\phi(x) = \int d^2\mathbf{k}_\perp |\psi(x, k_\perp)|^2$ is not the ‘‘true’’ parton distribution since only the lowest Fock state is considered and the normalization condition is not satisfied ($\int_0^1 \phi(x)dx < 1$). Employing the above wave functions and assuming $\psi_\pi(x, k_\perp) = \psi_\rho(x, k_\perp) = \psi_\omega(x, k_\perp)$, we can obtain the following relations between the polarized anti-quark distributions and the interference distributions:

$$\begin{aligned} \Delta\bar{d}_{\rho^+} &= \Delta\bar{u}_{\rho^-} = 2\Delta\bar{d}_{\rho^0} = 2\Delta\bar{u}_{\rho^0} = 2\Delta\bar{d}_\omega = 2\Delta\bar{u}_\omega \\ &= \phi(x), \\ \Delta\bar{d}_{\rho^0\omega} &= -\Delta\bar{u}_{\rho^0\omega} = -\frac{1}{2}\phi(x), \\ \Delta\bar{d}_{(\pi^+\rho^+)_0} &= \Delta\bar{u}_{(\pi^-\rho^-)_0} = 2\Delta\bar{d}_{(\pi^0\rho^0)_0} = 2\Delta\bar{u}_{(\pi^0\rho^0)_0} \\ &= \phi(x), \\ \Delta\bar{d}_{(\pi^0\omega)_0} &= -\Delta\bar{u}_{(\pi^0\omega)_0} = -\frac{1}{2}\phi(x). \end{aligned} \quad (13)$$

Although the above relations are derived from the quark model and by considering only the lowest Fock states, we

will assume they hold for the full wave function. Thus the distribution $\phi(x)$ can be replaced with the polarized parton distribution $\Delta v_\rho = \Delta\bar{d}_{\rho^+} = \Delta\bar{u}_{\rho^-}$ which, in principle, can be measured experimentally. We adopt two prescriptions to obtain the Δv_ρ :

- (i) employing the MIT bag model, and
- (ii) adopting the ansatz used in [13], i.e. relating it to the valence quark distribution of the π meson inspired by the lattice calculation of the first moments of the polarized and unpolarized parton distributions of the ρ meson.

We will consider the fluctuations $p \rightarrow N\pi, N\rho, N\omega$ and $p \rightarrow \Delta\pi, \Delta\rho$. We neglect the fluctuation $p \rightarrow \Delta\omega$ as this fluctuation is forbidden by isospin. The following relations exist for the fluctuation functions [21],

$$\begin{aligned} \Delta f_{\rho^+n/p} &= 2\Delta f_{\rho^0p/p} = \frac{2}{3}\Delta f_{\rho N/N}, \\ \Delta f_{\rho^-\Delta^{++}/p} &= \frac{3}{2}\Delta f_{\rho^0\Delta^+/p} = 3\Delta f_{\rho^+\Delta^0/p} = \frac{1}{2}\Delta f_{\rho\Delta/N}, \\ f_{(\pi^+\rho^+)n/p} &= 2f_{(\pi^0\rho^0)p/p} = f_{(\pi\rho)N/N}, \\ f_{(\pi^-\rho^-\Delta^{++}/p} &= \frac{3}{2}f_{(\pi^0\rho^0)\Delta^+/p} = 3f_{(\pi^+\rho^+)\Delta^0/p} \\ &= \frac{1}{2}f_{(\pi\rho)\Delta/N}. \end{aligned} \quad (14)$$

Using (13) and (14) we can obtain from (9),

$$\begin{aligned} x(\Delta\bar{d} - \Delta\bar{u}) &= \left[\frac{2}{3}\Delta f_{\rho N/N} - \frac{1}{3}\Delta f_{\rho\Delta/N} \right] \otimes \Delta v_\rho + \left[-\Delta f_{(\rho^0\omega)p/p} \right. \\ &\quad \left. + \frac{2}{3}f_{(\pi\rho)N/N}^0 - \frac{1}{3}f_{(\pi\rho)\Delta/N}^0 - f_{(\pi^0\omega)p/p}^0 \right] \otimes \Delta v_\rho \\ &= \Delta f_\rho \otimes \Delta v_\rho + \Delta f_{\text{int}} \otimes \Delta v_\rho. \end{aligned} \quad (15)$$

The first term is the same as the result given in [13]. We note that there are no contributions directly from the ω meson due to its charge structure. The second term is the interference contribution.

Now we turn to the calculation of the fluctuation functions. The fluctuation $N \rightarrow MB$ is described by the effective interaction Lagrangians [6],

$$\begin{aligned} \mathcal{L}_{NN\pi} &= ig_{NN\pi}\bar{N}\gamma_5\pi N, \\ \mathcal{L}_{N\Delta\pi} &= f_{N\Delta\pi}\bar{N}\partial_\mu\pi\Delta^\mu + \text{h.c.}, \\ \mathcal{L}_{NNV} &= g_{NNV}\bar{N}\gamma_\mu\theta^\mu N + f_{NNV}\bar{N}\sigma_{\mu\nu}N(\partial^\mu\theta^\nu - \partial^\nu\theta^\mu), \\ \mathcal{L}_{N\Delta\rho} &= f_{N\Delta\rho}i\bar{N}\gamma_5\gamma_\mu\Delta_\nu(\partial^\mu\theta^\nu - \partial^\nu\theta^\mu) + \text{h.c.}, \end{aligned} \quad (16)$$

where N is a spin-1/2 field, Δ a spin-3/2 field of Rarita-Schwinger form, π a pseudoscalar field, and θ a vector field. The coupling constants are taken to be [6, 22]

$$\begin{aligned} g_{NN\pi}^2/4\pi &= 13.6, \\ g_{NN\rho}^2/4\pi &= 0.84, \\ f_{NN\rho}/g_{NN\rho} &= 6.1/4m_N, \\ g_{NN\omega}^2/4\pi &= 8.1, \end{aligned}$$

$$\begin{aligned}
f_{NN\omega}/g_{NN\omega} &= 0, \\
f_{N\Delta\pi}^2/4\pi &= 12.3 \text{ GeV}^{-2}, \\
f_{N\Delta\rho}^2/4\pi &= 34.5 \text{ GeV}^{-2}.
\end{aligned} \tag{17}$$

The amplitudes $\phi_{MB}^{\lambda\lambda'}(y, k_{\perp}^2)$ which essentially determine the fluctuation function (see (3)) are calculated by using time-ordered perturbation theory in the infinite momentum frame,

$$\begin{aligned}
\phi_{MB}^{\lambda\lambda'}(y, k_{\perp}^2) &= \frac{1}{2\pi\sqrt{y(1-y)}} \\
&\times \frac{\sqrt{m_N m_B} V_{IMF}^{\lambda\lambda'}(y, k_{\perp}^2) G_{MB}(y, k_{\perp}^2)}{m_N^2 - m_{MB}^2(y, k_{\perp}^2)}, \tag{18}
\end{aligned}$$

where m_{MB}^2 is the invariant mass squared of the MB Fock state,

$$m_{MB}^2(y, k_{\perp}^2) = \frac{m_M^2 + k_{\perp}^2}{y} + \frac{m_B^2 + k_{\perp}^2}{1-y}. \tag{19}$$

As usual a phenomenological vertex form factor, $G_{MB}(y, k_{\perp}^2)$, is introduced to describe the unknown dynamics of the fluctuation $N \rightarrow MB$. Here we adopt the exponential form,

$$G_{MB}(y, k_{\perp}^2) = \exp\left[\frac{m_N^2 - m_{MB}(y, k_{\perp}^2)}{2\Lambda^2}\right], \tag{20}$$

where Λ is a cut-off parameter. We adopt $\Lambda_{\text{oct}} = 1.08 \text{ GeV}$ and $\Lambda_{\text{dec}} = 0.98 \text{ GeV}$ for the fluctuations involving the octet and decuplet baryons respectively [6]. This form factor satisfies the relation $G_{MB}(y, k_{\perp}^2) = G_{BM}(1-y, k_{\perp}^2)$.

We note that there are two prescriptions for calculating the vertex functions V_{IMF} , depending on the manner in which the meson energy is treated. In this work we follow the prescription used in [6], i.e. the meson energy in the vertex is $E_N - E_B$, which is called method (B) in [13]. The expressions for the various fluctuation functions in (15) are given in the appendix. These expressions agree with the vertex functions given in [6], but differ from those given in the appendix of [13] in the following ways:

- (1) The terms proportional to $f_{NN\rho} g_{NN\rho}$ in $f_{\rho N/N}^{\lambda}(y)$ have the opposite sign;
- (2) Our results for $f_{\rho\Delta/N}^{\lambda}(y)$ agree with the results of method (A) in [13] ((24) and (26) in the appendix of [13]), rather than the results of method (B). Finally, we note that adopting the alternative method (method (A) of [13]) leads to somewhat smaller values of $(\Delta\bar{d} - \Delta\bar{u})$, but does not change our conclusions significantly.

There is little experimental information on the parton distributions of the vector meson. Although it is common practice to set the unpolarized parton distribution of the ρ meson equal to that of the pion, the study of the polarized parton distribution of the ρ meson is lacking both in experiment and theory. The lattice calculation [23] finds that the polarization of the ρ meson is about 60%. So the ansatz $\Delta v_{\rho}(x) = 0.6v_{\pi}(x)$ was used in [13]. We note that the lattice prediction of 60% polarization is for the ratio

of the first moments of the polarized and unpolarized parton distributions, i.e. $\int_0^1 \Delta v_{\rho}(x) dx = 0.6 \int_0^1 v_{\rho}(x) dx$ and it is quite possible that the x -dependence of the polarized parton distribution may be different from that of the unpolarized one.

As an alternative hypothesis for the x -dependence of the polarized parton distribution, we employ a non-perturbative model of hadrons, the MIT bag model [24]. The bag model has been shown to be a useful tool in the study of the non-perturbative structure of hadrons (e.g., mass spectrum, parton distribution). The theoretical calculations [25–27] of the parton distributions of the nucleon, including meson cloud contributions, can give results consistent with the experimental data.

An interesting aspect of the bag model calculation is that it can be generalized to provide useful information on the parton distributions of the other hadrons. The parton distributions for both polarized and unpolarized octet and decuplet baryons have been calculated in the bag model [18]. However, most present bag model calculations for the parton distributions are for the baryons. There has been no attempt in the bag model to calculate the parton distributions of the mesons. This is due, at least in part, to the lack of experimental data on the parton distributions of the mesons¹. While the bag model is probably not very applicable to the pion, it does describe the rest of the pseudoscalar nonet and the vector octet reasonably well. So adapting the methods used to calculate baryon parton distributions to the meson sector should give a useful approximation to the parton distributions of the mesons, in particular the ρ meson.

Adapting the argument of [27] we obtain the expression for the quark distribution function in a ρ meson, where we include only one-quark intermediate states

$$\begin{aligned}
q_{\rho, f}^{\uparrow\downarrow}(x) &= \frac{M_{\rho}}{(2\pi)^3} \sum_m \langle \mu | P_{f, m} | \mu \rangle \int d\mathbf{p}_n \frac{|\phi_1(\mathbf{p}_n)|^2}{|\phi_2(\mathbf{0})|^2} \\
&\times \delta(M_{\rho}(1-x) - p_n^+) |\tilde{\Psi}_{+, f}^{\uparrow\downarrow}(\mathbf{p}_n)|^2. \tag{21}
\end{aligned}$$

Here $+$ components of momenta are defined by $p^+ = p^0 + p^3$, \mathbf{p}_n is the 3-momentum of the intermediate state, $\tilde{\Psi}$ is the Fourier transform of the MIT bag ground state wave function $\Psi(\mathbf{r})$, and $\phi_m(\mathbf{p})$ is the Fourier transform of the Hill–Wheeler overlap function between m -quark bag states:

$$|\phi_m(\mathbf{p})|^2 = \int d\mathbf{R} e^{-i\mathbf{p}\cdot\mathbf{R}} \left[\int d\mathbf{r} \Psi^{\dagger}(\mathbf{r} - \mathbf{R}) \Psi(\mathbf{r}) \right]^m. \tag{22}$$

The ϕ functions arise through the use of the Peierls-Yoccoz projection to form momentum eigenstates from the initial and intermediate bag states. The matrix element $\langle \mu | P_{f, m} | \mu \rangle$ appearing in (21) is the matrix element of the projection operator $P_{f, m}$ onto the required flavor f and helicity m for the $SU(6)$ spin-flavor wave function $|\mu\rangle$ of the ρ meson.

¹ At present only the parameterization for the parton distributions of the pion has been extracted experimentally [28]

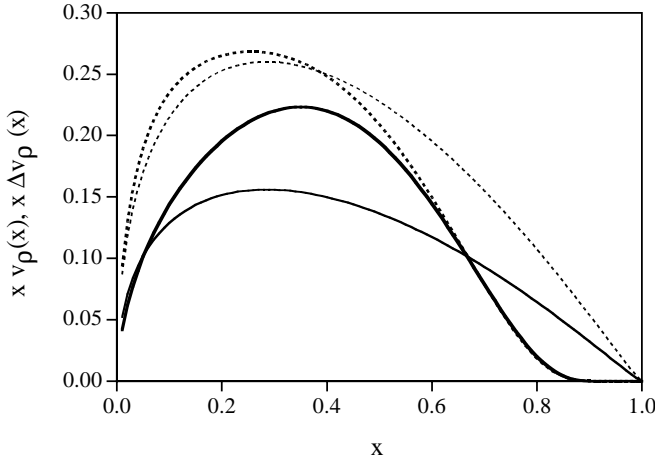


Fig. 2. The polarized and unpolarized valence quark distributions of the ρ meson at $Q^2 = 4 \text{ GeV}^2$. The thick dashed and solid curves are the bag model calculations for the unpolarized and polarized distributions respectively. The thin dashed curve is the unpolarized parton distribution of the π meson [29]. The thick solid curve is the polarized parton distribution of the ρ meson using the ansatz $\Delta v_\rho(x) = 0.6v_\pi(x)$ [13]

3 Results and discussion

We first fix the parameters of the MIT bag model calculation by fitting the calculated unpolarized parton distribution of the ρ meson to the Glück–Reya–Schienbein parameterization (GRS99) [29] for the valence parton distribution of the pion², which is essentially fixed by the π - N Drell–Yan data. For the parton distributions of the nucleon, the bag model calculations with only two-quark intermediate states are usually smaller than the data in the small x region and do not satisfy the normalization condition of the probability, i.e. $P_2 < 1$ rather than $P_2 = 1$ [25–27]. It is necessary to include intermediate states with three quarks and one anti-quark, arising from the action of the field operator ($\psi = b + d^\dagger$) on the three-quark bag state. This allows the normalization condition to be satisfied. Such contributions from multi-quark intermediate states can be well parameterized by the form $f_4(x) = N_4(1-x)^7$ consistent with the Drell–Yan–West relation [27]. For simplicity we will employ a similar function form, $f_3(x) = N_3(1-x)^5$, to parameterize the three-quark (and two-quark plus one-anti-quark) intermediate state contributions to the unpolarized parton distributions of the ρ meson. The value of N_3 is determined from the normalization condition $P_1 + P_3 = 1$, where P_1 and P_3 are the probabilities of the one-quark and three-quark intermediate states respectively. The parameters needing to be fixed are the radius of the bag R , the mass of the one-quark intermediate state m_1 , and the low momentum scale μ^2 , at which the model is supposed to be valid. The next-to-leading-order GRS99 parameterization is given at a scale $\mu_{\text{NLO}}^2 = 0.40 \text{ GeV}^2$:

² As usual we take the unpolarized pion and ρ valence distributions to be the same

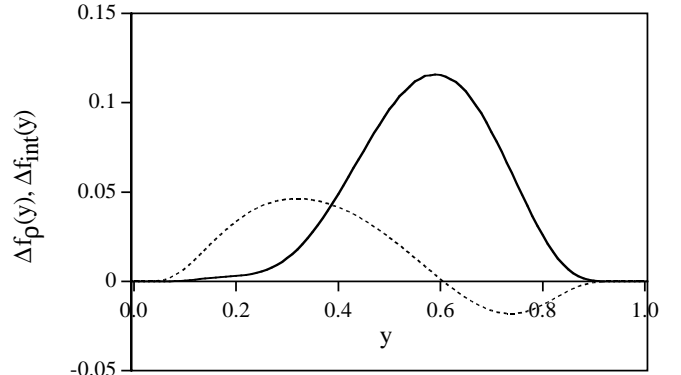


Fig. 3. The polarized fluctuation functions for the vector meson (the solid curve) and the interference terms (the dashed curve)

$$v_{\text{NLO}}^\pi(x, \mu_{\text{NLO}}^2) = 0.696x^{-0.447}(1-x)^{0.426}, \quad (23)$$

where $v^\pi = u_v^{\pi^+} = \bar{d}_v^{\pi^+}$. Both the GRS99 parton distributions and our calculations are evolved to the scale $Q^2 = 4 \text{ GeV}^2$ and the results are shown in Fig. 2. The thin dashed curve is the GRS99 parameterization, and the thick dashed curve is the bag model calculation. A good agreement in the small and intermediate x region is found for $R = 0.7 \text{ fm}$, $m_1 = 0.55m_\rho$, $N_3 = 1.68$ and $\mu^2 = 0.23 \text{ GeV}^2$.

Having fixed the parameters we calculate the polarized parton distribution of the ρ , $x\Delta v_\rho^{\text{MIT}}(x)$. The result is presented in Fig. 2 as the thick solid curve. The first moment of $\Delta v_\rho^{\text{MIT}}(x)$ is found to be about 0.60 at $Q^2 = 4 \text{ GeV}^2$, which is in agreement with the lattice value of 0.60. For comparison, the distribution $0.6xv_\pi(x)$, which could be set as the polarized parton distribution according to the ansatz used in [13], is also shown in Fig. 2 as the thin solid curve. It can be seen that the distribution $0.6xv_\pi(x)$ is smaller than the bag model calculation $x\Delta v_\rho^{\text{MIT}}(x)$ in the intermediate x region, although both distributions satisfy the same normalization condition. Also the bag model polarized parton distribution has a different x -dependence from the unpolarized distribution.

We show the polarized fluctuation functions of the ρ meson (Δf_ρ in (15), the solid curve) and the interference terms (Δf_{int} in (15), the dashed curve) in Fig. 3. It can be seen that the maximum of Δf_{int} is about 40% of that of Δf_ρ and that Δf_{int} changes sign from positive to negative at about $y = 0.6$. So the contribution to $\Delta\bar{d} - \Delta\bar{u}$ from the interference terms is not negligible.

As we have discussed in the last section, our expressions for $f_{\rho N/N}^\lambda$ and $f_{\rho\Delta/N}^\lambda$ are different from those given in [13]. We show the numerical difference in Fig. 4, where the fluctuation functions $\Delta f_{\rho NN}$ (dashed curves), $\Delta f_{\rho\Delta N}$ (dotted curves), and $\Delta f_\rho = (2/3)\Delta f_{\rho NN} - (1/3)\Delta f_{\rho\Delta N}$ (solid curves) which enter directly in the calculation of $\Delta\bar{d} - \Delta\bar{u}$ (see (15)) are plotted. The thick curves are our results, while the thin curves are from [13]. In each case the cut-off parameter in the form factor has been set to the same value $\Lambda_{\text{Oct}} = \Lambda_{\text{Dec}} = 0.85 \text{ GeV}$. The difference is about 50%.

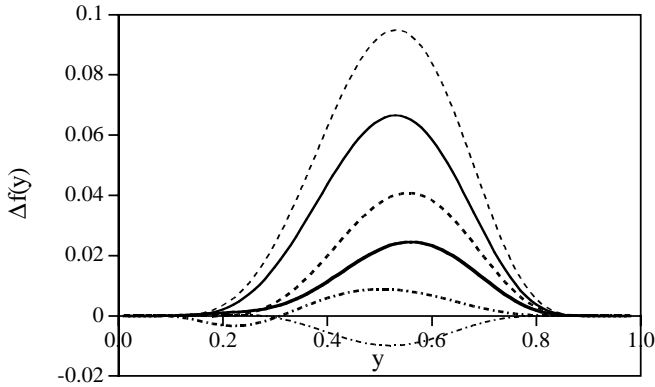


Fig. 4. Comparison of polarized fluctuation functions, $\Delta f_{\rho NN}$ (dashed curves), $\Delta f_{\rho \Delta N}$ (dashed-dotted curves), and $(2/3)\Delta f_{\rho NN} - (1/3)\Delta f_{\rho \Delta N}$ (solid curves), given in this work (thick curves) and in [13] (thin curves)

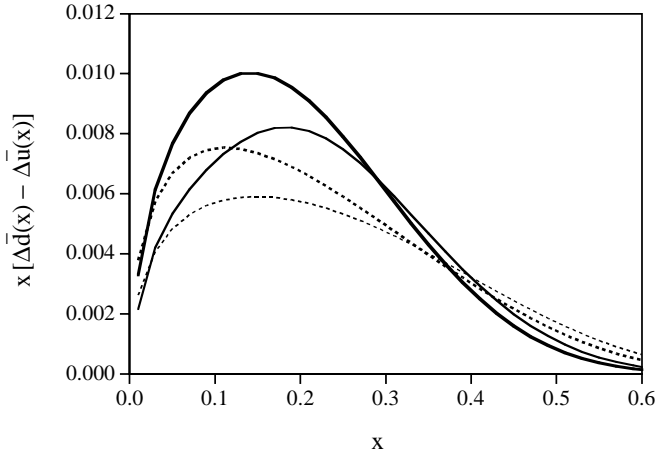


Fig. 5. The flavor asymmetry of the anti-quark in the proton. The solid curves are the predictions using $x\Delta v_{\rho}^{\text{MIT}}(x)$, while the dashed curves are obtained by using $0.6xv_{\pi}(x)$. The thin curves are the results without interference terms, while the thick curves are the results with interference terms

We calculate the flavor asymmetry of the polarized anti-quark distributions employing both the bag model distribution $x\Delta v_{\rho}^{\text{MIT}}(x)$ and $0.6xv_{\pi}(x)$ for the polarized valence parton distribution of the ρ meson. The results are shown in Fig. 5. The solid curves are the predictions using $x\Delta v_{\rho}^{\text{MIT}}(x)$, while the dashed curves are obtained by using $0.6xv_{\pi}(x)$. The thin curves are the results without interference terms while the thick curves are the results with interference terms. We see that the interference effect mildly increases the predictions for the flavor asymmetry, and pushes the curves towards the small x region due to Δf_{int} being peaked at smaller y ($y_{\text{max}} \simeq 0.3$) than the Δf_{ρ} ($y_{\text{max}} \simeq 0.60$). For the calculations with $x\Delta v_{\rho}^{\text{MIT}}(x)$, the asymmetry with interference terms included exhibits a maximum at $x \simeq 0.12$, while the asymmetry without interference terms exhibits a maximum at $x \simeq 0.18$. Also it can be seen that the calculations with $x\Delta v_{\rho}^{\text{MIT}}(x)$ (the solid curves) are larger than that with $0.6xv_{\pi}(x)$ (the dashed

curves) in the intermediate x region, and have their maxima at larger x .

The integral

$$I_{\Delta} = \int_0^1 dx [\Delta \bar{d}(x) - \Delta \bar{u}(x)] \\ = \int_0^1 dx \Delta v_{\rho}(x) \int_0^1 dy [\Delta f_{\rho}(y) + \Delta f_{\text{int}}(y)] \quad (24)$$

will be the same for both models for the polarized parton distribution of the ρ as they have the same first moment for the polarized distribution. We find the integral to be 0.023 (0.031) without (with) the interference terms. The interference effect increases the integral by about 30%.

Using a softer form factor for the octet contributions, as suggested by the fit of $\bar{d}(x) - \bar{u}(x)$ at large x [21], will lower the value of the integral I_{Δ} . For example, taking $\Lambda_{\text{oct}} = 0.80$ GeV and $\Lambda_{\text{dec}} = 1.0$ GeV consistent with the analysis of [21], the integral decreases to -1.1×10^{-4} ($+5.7 \times 10^{-3}$) without (with) the interference terms. In this case the flavor asymmetry between \bar{d} and \bar{u} is very small. The reason is that the fluctuation $p \rightarrow \Delta\rho$ gives a negative contribution to the integral I_{Δ} and this fluctuation is greatly emphasized for the above cut-off parameters³. The prediction for the integral I_{Δ} has a strong dependence on the cut-off parameters Λ_{oct} and Λ_{dec} . For example, the results calculated including interference terms vary from 0.0043 to 0.033 for the cut-off parameters changing from $\Lambda_{\text{oct}} = \Lambda_{\text{dec}} = 0.8$ GeV to 1.10 GeV. Clearly these values obtained using the meson cloud model are very different from those obtained using the chiral quark-soliton model [12] which have a magnitude of around 0.3. It is interesting that both models agree well with the experimental data for the unpolarized asymmetry, yet predict very different results for the polarized asymmetry. As the magnitude of the predicted polarized asymmetry appears to be fairly natural in each of these models, experimental data will provide a valuable test of these models, and give insight into the relation between helicity dependent and helicity independent observables in quark models.

We do not find that the π - ρ interference terms can be sizable, which appears to be in disagreement with the conclusions of Boreskov and Kaidalov [14]. The main reason for this disagreement is that we do not here consider interference terms where the ρ meson has non-zero helicity. This is because any such terms only contribute to amplitudes in the virtual Compton scattering which have a spin-flip between the incoming and outgoing proton states. These spin-flip amplitudes in turn only contribute to the cross-section σ_1 , which is the interference between transverse and longitudinal polarizations of the virtual photon [31]:

$$\sigma_1 \propto \frac{\sqrt{Q^2}}{M^2} \left[G_1 + \frac{\nu}{M} G_2 \right]$$

³ The probabilities for $p \rightarrow N\rho$ and $p \rightarrow \Delta\rho$ are 0.012 and 0.042 respectively, while the probabilities are 0.189 and 0.034 for the parameter values $\Lambda_{\text{oct}} = 1.08$ GeV and $\Lambda_{\text{dec}} = 0.98$ GeV

$$\rightarrow \frac{\sqrt{Q^2}}{M\nu} [g_1(x) + g_2(x)] \text{ in the Bjorken limit.} \quad (25)$$

So any interference terms involving non-zero helicity ρ mesons can be expected to decrease as $1/\sqrt{Q^2}$ as Q^2 gets large. Using the operator product expansion shows that the relevant operators are all twist 3 or higher. As the experimental data for $g_1(x)$ for both the proton and the neutron show no marked Q^2 dependence, we conclude that these higher twist contributions are not relevant at the experimental scales.

4 Pauli blocking contributions to the flavor asymmetry

We have not so far considered any contribution to the asymmetry arising from ‘‘Pauli blocking’’ effects [21, 25, 32]. In a model such as the bag model, where the valence quarks are confined by a scalar field, the vacuum inside a hadron is different from the vacuum outside. This manifests itself as a distortion in the negative energy Dirac sea, which is full for the outside (or free) vacuum, whereas there will be empty states in the Dirac sea of the bag. To an external probe this change in vacuum structure appears as an intrinsic, non-perturbative sea of $q\bar{q}$ pairs [33]. This change in the vacuum is similar to the change in the Fermi–Dirac distribution when the temperature is increased to above absolute zero. Now when a quark is put into the ground state of the bag it will have the effect of filling some of the empty negative energy states in the sea of the bag vacuum. The reason for this is that the ground state wave function can be written as a wave packet in terms of plane wave states of positive and negative energy, with the energy distribution of the wave packet centred at the ground state energy eigenvalue, but with non-zero contributions from negative energy plane waves. Hence the presence of a quark in the bag ground state lowers the probability of a negative energy state being empty, which is the same as lowering the probability of finding a positive energy anti-quark. As the proton consists of two up quarks and one down quark, the probability of finding a \bar{u} anti-quark is reduced more than the probability of finding a \bar{d} anti-quark i.e. $\bar{d} > \bar{u}$. The analysis of [21] showed that, in the context of the meson cloud model, about 50% of the observed $\bar{d}-\bar{u}$ asymmetry may be due to Pauli blocking.

When we include spin in the analysis of Pauli blocking, we find that putting a spin up quark into the bag ground state has the effect of filling some of the negative energy spin up quark states in the bag vacuum, which is equivalent to lowering the probability of finding a positive energy spin down anti-quark. As the $SU(6)$ wave function of the spin up proton is dominated by terms with the two up quarks having spin parallel to the proton spin and the down quark having spin anti-parallel, Pauli blocking predicts that the probabilities of finding spin down \bar{u} anti-quarks and spin up \bar{d} anti-quarks are reduced i.e. $\bar{u}^\uparrow > \bar{u}^\downarrow$, $\bar{d}^\downarrow > \bar{d}^\uparrow$ or $\Delta\bar{u}(x) \geq 0$, $\Delta\bar{d}(x) \leq 0$.

We can also estimate the contribution of the Pauli blocking effect to the polarized asymmetry, again using

the Adelaide group’s argument for calculating parton distributions in the bag model. In the parton model, the anti-quark distribution functions are given by

$$\bar{q}^{\uparrow\downarrow}(x) = p^+ \sum_n \delta(p^+(1-x) - p_n^+) \times \left| \langle n | \frac{1}{2}(1 \mp \gamma^5) \Psi^\dagger(0) | p, s \rangle \right|^2. \quad (26)$$

The appropriate intermediate state $|n\rangle$ consists of four quarks. If we assume the $SU(6)$ wave function for the proton with spin $+1/2$, and insert an additional quark only into the radial ground state, then we have the following matrix elements for the projection operators onto spin and flavor [27]

$$\begin{aligned} \langle \mu | P_{u,+1/2}^{(q)} | \mu \rangle &= \frac{4}{3}, & \langle \mu | P_{u,-1/2}^{(q)} | \mu \rangle &= \frac{8}{3}, \\ \langle \mu | P_{d,+1/2}^{(q)} | \mu \rangle &= \frac{8}{3}, & \langle \mu | P_{d,-1/2}^{(q)} | \mu \rangle &= \frac{7}{3}. \end{aligned} \quad (27)$$

We have ignored any effects of spin–spin coupling in the intermediate state. Following the argument of the Adelaide group for calculating the parton distributions we can then write the anti-quark distributions as

$$\begin{aligned} \bar{u}^{\uparrow\downarrow} &= 2F_{(4)}(x) \pm \frac{2}{3}G_{(4)}(x), \\ \bar{d}^{\uparrow\downarrow} &= \frac{5}{2}F_{(4)}(x) \mp \frac{1}{6}G_{(4)}(x), \end{aligned} \quad (28)$$

where $F_{(4)}(x)$ and $G_{(4)}(x)$ are the spin independent and spin dependent kinematic integrals over the momentum of the intermediate four quark state. The sea asymmetries can then be expressed as

$$\begin{aligned} \bar{d}(x) - \bar{u}(x) &= F_{(4)}(x), \\ \Delta\bar{d}(x) - \Delta\bar{u}(x) &= -\frac{5}{3}G_{(4)}(x). \end{aligned} \quad (29)$$

As $G_{(4)}(x)$ is positive at all x , Pauli blocking gives a negative contribution to the spin dependent flavor asymmetry in the sea, whereas the meson cloud contribution tended to be positive. Also noting that as $F_{(4)}(x) \geq G_{(4)}(x)$, we can integrate over all x and then obtain an upper limit for the size of the Pauli blocking contribution to the spin dependent asymmetry in terms of the contribution to the spin independent asymmetry:

$$-\int_0^1 dx [\Delta\bar{d}(x) - \Delta\bar{u}(x)] \leq \frac{5}{3} \int_0^1 dx [\bar{d}(x) - \bar{u}(x)]. \quad (30)$$

As an estimate for the integral on the r.h.s. of (30) we may use the value of 0.07 given by the analysis of [21]. This then gives an upper limit of about 0.12 for the magnitude of the integral over the polarized asymmetry. In the bag model, the ratio $G_{(4)}(x)/F_{(4)}(x)$ varies from about 0.8 at low x to unity at large x , which gives us a value of about -0.09 for the integrated polarized asymmetry. While these values are calculated at some scale appropriate to the bag model, the values of the integrals are not

much affected by evolution up to experimental scales, so we expect the relation between polarized and unpolarized sea asymmetries to be approximately correct at all scales. The value of the Pauli blocking contribution to the integrated polarized asymmetry is much larger than that we have calculated in the meson cloud model, in contrast to the approximate equality in the unpolarized case. Thus the experimental observation of any asymmetry in the polarized sea distributions is much more a test of the Pauli blocking hypothesis than of the meson cloud model.

The Bjorken sum rule may be written

$$\begin{aligned} & \int_0^1 dx [g_1^p(x) - g_1^n(x)] \\ &= \frac{1}{6} \int_0^1 dx [(\Delta u(x) - \Delta d(x)) + (\Delta \bar{u}(x) - \Delta \bar{d}(x))] \\ &= \frac{1}{6} \left| \frac{g_A}{g_V} \right| \left(1 - \frac{\alpha_s}{\pi} \right). \end{aligned} \quad (31)$$

We estimate that the contribution to the sum rule from Pauli blocking plus meson cloud effects is about 5–10% of the value of the sum rule.

We note that the Dortmund group have recently [34] analyzed the polarized sea asymmetry also using a Pauli blocking type ansatz, and found a value around -0.3 for the integrated asymmetry. This would correspond to a contribution of around 20% to the Bjorken sum rule. The Dortmund analysis was based on the proposed relation between polarized distributions:

$$\frac{\Delta \bar{d}(x)}{\Delta \bar{u}(x)} = \frac{\Delta u(x)}{\Delta d(x)}. \quad (32)$$

This relation is not obeyed by the distributions in our analysis. The reason for this is that Pauli blocking should most affect the $\Delta \bar{u}$ distribution rather than the $\Delta \bar{d}$ distribution (starting from an assumed $SU(6)$ value of 0), and hence the l.h.s. of the relation (32) has a magnitude less than one, while the magnitude of the r.h.s. is greater than one.

5 Summary

The meson cloud model is very successful in explaining the flavor asymmetry of the unpolarized parton distributions in the nucleon sea. In this paper, we have calculated the flavor asymmetry for the polarized anti-quark distributions of the nucleon. We have included the contributions from both the vector meson cloud and the interference terms between pseudoscalar and vector mesons. We have used two prescriptions to describe the polarized valence quark distribution of the ρ meson:

- (i) calculating it in the bag model and
- (ii) employing the ansatz given in [13] to relate it to the unpolarized quark distribution of the π meson. Our calculations show that the interference effect mildly increases the prediction for $\Delta \bar{d}(x) - \Delta \bar{u}(x)$ in the intermediate x region. We have also discussed the effect of ‘‘Pauli blocking’’ on the asymmetry, and we have seen that this effect

gives a larger contribution to the asymmetry than meson cloud effects, in contrast to the unpolarized case.

Acknowledgements. We would like to thank Tony Thomas, Wally Melnitchouk, Andreas Schreiber and Kazuo Tsushima for a number of useful discussions, especially in regard to the sign of Pauli blocking contributions to the polarized sea asymmetry. Part of this work was carried out while the authors were guests at the Centre for the Subatomic Structure of Matter at the University of Adelaide. This work was partially supported by the Science and Technology Postdoctoral Fellowship of the Foundation for Research Science and Technology, and the Marsden Fund of the Royal Society of New Zealand.

Appendix

We give here expressions for the helicity dependent fluctuation functions appearing in (15), where the superscript 1 (−1) is the vector meson helicity.

$$\Delta f_{\rho N/N} = f_{\rho N/N}^1 - f_{\rho N/N}^{-1}, \quad (33)$$

$$\begin{aligned} & f_{\rho N/N}^1(y) \\ &= \frac{3}{8\pi^2(-1+y)^2 y^3} \int_0^\infty \frac{dk_\perp^2 G_{\rho N}^2(y, k_\perp^2)}{[m_N^2 - m_{\rho N}^2(y, k_\perp^2)]^2} \\ & \times \left\{ g_{NN\rho}^2 (k^2 + m_N^2 y^4) \right. \\ & + 4f_{NN\rho}^2 (k^4 + 5k^2 m_N^2 y^2 + 4m_N^4 y^4) \\ & \left. - 4f_{NN\rho} g_{NN\rho} m_N y [2m_N^2 y^3 + k^2(1+y)] \right\}, \end{aligned} \quad (34)$$

$$\begin{aligned} & f_{\rho N/N}^{-1}(y) \\ &= \frac{3}{8\pi^2(-1+y)^2 y^3} \int_0^\infty \frac{dk_\perp^2 G_{\rho N}^2(y, k_\perp^2)}{[m_N^2 - m_{\rho N}^2(y, k_\perp^2)]^2} \\ & \times \left\{ k^2 [g_{NN\rho}^2 (-1+y)^2 - 4f_{NN\rho} g_{NN\rho} m_N \right. \\ & \left. \times (-1+y)y + 4f_{NN\rho}^2 (k^2 + m_N^2 y^2)] \right\}, \end{aligned} \quad (35)$$

$$\Delta f_{\rho \Delta/N}(y) = f_{\rho \Delta/N}^1(y) - f_{\rho \Delta/N}^{-1}(y), \quad (36)$$

$$\begin{aligned} & f_{\rho \Delta/N}^1(y) \\ &= \frac{f_{N\Delta\rho}^2}{24m_\Delta^2 \pi^2 (-1+y)^4 y^3} \int_0^\infty \frac{dk_\perp^2 G_{\rho\Delta}^2(y, k_\perp^2)}{[m_N^2 - m_{\rho\Delta}^2(y, k_\perp^2)]^2} \\ & \times \left\{ k^6 + k^4 m_\Delta^2 (3 - 4y + 4y^2) + k^2 m_\Delta y \right. \\ & \times \left[-4m_N m_\rho^2 (-1+y)^3 + m_\Delta^3 y (4 - 4y + 3y^2) \right] \\ & \left. + [m_N m_\rho^2 (-1+y)^3 + m_\Delta^3 y^2]^2 \right\}, \end{aligned} \quad (37)$$

$$\begin{aligned} & f_{\rho \Delta/N}^{-1}(y) \\ &= \frac{f_{N\Delta\rho}^2}{24m_\Delta^2 \pi^2 (-1+y)^2 y^3} \int_0^\infty \frac{dk_\perp^2 G_{\rho\Delta}^2(y, k_\perp^2)}{[m_N^2 - m_{\rho\Delta}^2(y, k_\perp^2)]^2} \end{aligned}$$

$$\begin{aligned} & \times \left\{ k^4 m_N^2 + k^2 [m_\rho^2 (-1 + y) + 2m_\Delta m_N y]^2 \right. \\ & \left. + 3m_\Delta^2 [m_\rho^2 (-1 + y) + m_\Delta m_N y]^2 \right\}, \end{aligned} \quad (38)$$

$$\Delta f_{(\rho^0\omega)p/p} = f_{(\rho^0\omega)p/p}^1 - f_{(\rho^0\omega)p/p}^{-1}, \quad (39)$$

$$\begin{aligned} & f_{(\rho^0\omega)p/p}^1(y) \\ &= \frac{3g_{NN\omega}}{8\pi^2(-1+y)^2 y^3} \\ & \times \int_0^\infty \frac{dk_\perp^2 G_{\rho N}(y, k_\perp^2) G_{\omega N}(y, k_\perp^2)}{[m_N^2 - m_{\rho N}^2(y, k_\perp^2)][m_N^2 - m_{\omega N}^2(y, k_\perp^2)]} \\ & \times \left\{ g_{NN\rho} (k^2 + m_N^2 y^4) \right. \\ & \left. - 2f_{NN\rho} m_N y [2m_N^2 y^3 + k^2 (1 + y)] \right\}, \end{aligned} \quad (40)$$

$$\begin{aligned} & f_{(\rho^0\omega)p/p}^{-1}(y) \\ &= \frac{3g_{NN\omega}}{8\pi^2(-1+y)y^3} \\ & \times \int_0^\infty \frac{dk_\perp^2 G_{\rho N}(y, k_\perp^2) G_{\omega N}(y, k_\perp^2)}{[m_N^2 - m_{\rho N}^2(y, k_\perp^2)][m_N^2 - m_{\omega N}^2(y, k_\perp^2)]} \\ & \times \left\{ k^2 [g_{NN\rho} (-1 + y) - 2f_{NN\rho} m_N y] \right\}. \end{aligned} \quad (41)$$

For pseudoscalar–vector interference terms, only helicity zero contributes at leading twist.

$$\begin{aligned} & f_{(\pi\rho)N/N}^0(y) \\ &= \frac{3}{16m_\rho\pi^2(-1+y)^3 y^2} \\ & \times \int_0^\infty \frac{dk_\perp^2 G_{\pi N}(y, k_\perp^2) G_{\rho N}(y, k_\perp^2)}{[m_N^2 - m_{\pi N}^2(y, k_\perp^2)][m_N^2 - m_{\rho N}^2(y, k_\perp^2)]} \\ & \times \left\{ g_{NN\pi} [k^2 + m_\rho^2 (-1 + y) + m_N^2 y^2] \right\} \\ & \times \left\{ -g_{NN\rho} m_N (-1 + y) y \right. \\ & \left. + f_{NN\rho} [-k^2 (-2 + y) + m_N^2 y^3] \right\}, \end{aligned} \quad (42)$$

$$\begin{aligned} & f_{(\pi\rho)\Delta/N}^0(y) \\ &= \frac{f_{N\Delta\pi} f_{N\Delta\rho} m_\rho}{24m_\Delta\pi^2(-1+y)^3 y^2} \\ & \times \int_0^\infty \frac{dk_\perp^2 G_{\pi\Delta}(y, k_\perp^2) G_{\rho\Delta}(y, k_\perp^2)}{[m_N^2 - m_{\pi\Delta}^2(y, k_\perp^2)][m_N^2 - m_{\rho\Delta}^2(y, k_\perp^2)]} \\ & \times \left\{ k^4 (2 + y) - 2k^2 [2m_\Delta m_N (-1 + y) \right. \\ & \left. - m_N^2 (-1 + y)^2 (1 + y) + m_\Delta^2 (-1 + 2y)] \right. \\ & \left. + [m_\Delta^2 - m_N^2 (-1 + y)^2]^2 y \right\}, \end{aligned} \quad (43)$$

$$\begin{aligned} & f_{(\pi^0\omega)p/p}^0(y) \\ &= \frac{-3g_{NN\pi} g_{NN\omega} m_N}{16m_\omega\pi^2(-1+y)^2 y} \end{aligned}$$

$$\begin{aligned} & \times \int_0^\infty \frac{dk_\perp^2 G_{\pi N}(y, k_\perp^2) G_{\rho N}(y, k_\perp^2)}{[m_N^2 - m_{\pi N}^2(y, k_\perp^2)][m_N^2 - m_{\omega N}^2(y, k_\perp^2)]} \\ & \times [k^2 + m_\omega^2 (-1 + y) + m_N^2 y^2]. \end{aligned} \quad (44)$$

References

1. J. Ashman et al., Nucl. Phys. B **328**, 1 (1989)
2. P. Amaudraz et al., Phys. Rev. Lett. **66**, 2712 (1991); M. Arneodo et al., Phys. Rev. D **50**, R1 (1994); M. Arneodo et al., Phys. Lett. B **364**, 107 (1995)
3. A. Baldit et al., NA51 Collaboration, Phys. Lett. B **332**, 244 (1994)
4. E.A. Hawker et al., E866/NuSea Collaboration, Phys. Rev. Lett. **80**, 3715 (1998); hep-ex/0103030
5. A.W. Thomas, Phys. Lett. B **126**, 97 (1983)
6. H. Holtmann, A. Szczurek, J. Speth, Nucl. Phys. A **569**, 631 (1996)
7. J. Speth, A.W. Thomas, Adv. Nucl. Phys. **24**, 83 (1998)
8. S. Kumano, Phys. Rep. **303**, 103 (1998)
9. B. Adeva, SMC Collaboration, Phys. Lett. B **420**, 180 (1998); K. Ackerstaff, HERMES Collaboration, Phys. Lett. B **464**, 123 (1999); T. Morii, T. Yamanishi, hep-ph/9905294
10. M. Glück, E. Reya, M. Stratmann, W. Vogelsang, Phys. Rev. D **53**, 4775 (1996); T. Fehrmann, W.J. Stirling, Phys. Rev. D **53**, 6100 (1996); E. Leader, A.V. Sidorov, D.B. Stamenov, Phys. Rev. D **58**, 114028 (1998); Y. Goto et al., Asymmetry Analysis Collaboration, hep-ph/0001046; J. Bartelski, S. Tatur, hep-ph/0004251
11. D.I. Diakonv et al., Nucl. Phys. B **480**, 341 (1996); Phys. Rev. D **56**, 4069 (1997); P.V. Pobylitsa, M.V. Polyakov, Phys. Lett. B **389**, 350 (1996)
12. P.V. Pobylitsa et al., hep-ph/9804436; B. Dressler et al., hep-ph/9809487; 9909541; M. Wakamatsu, hep-ph/0010262
13. R.J. Fries, A. Schäfer, Phys. Lett. B **443**, 40 (1998); hep-ph/9805509
14. K.G. Boreskov, A.B. Kaidalov; Eur. Phys. J. C **10**, 143 (1999)
15. A.E. Dorokhov, N.I. Kochelev, Yu.A. Zubov, Int. J. Mod. Phys. A **8**, 603 (1993); A.E. Dorokhov, N.I. Kochelev, Phys. Lett. B **304**, 167 (1993)
16. R.S. Bhalerao, Phys. Rev. C **63**, 025208 (2001)
17. A.W. Schreiber, A.W. Thomas, Phys. Lett. B **215**, 141 (1988)
18. C. Boros, A.W. Thomas, Phys. Rev. D **60**, 074017 (1999)
19. A.W. Schreiber, P. Mulders, A.I. Signal, A.W. Thomas, Phys. Rev. D **45**, 3069 (1992); F.M. Steffens, H. Holtmann, A.W. Thomas, Phys. Lett. B **358**, 139 (1995)
20. F.E. Close, An introduction to quarks and partons (Academic Press Inc., 1979)
21. W. Melnitchouk, J. Speth, A.W. Thomas, Phys. Rev. D **59**, 014033 (1998)
22. R. Machleidt, K. Holinde, Ch. Elster, Phys. Rep. **149**, 1 (1987)
23. C. Best et al., Phys. Rev. D **56**, 2743 (1997)
24. See, e.g., T. DeGrand, R.L. Jaffe, K. Johnson, J. Kiskis, Phys. Rev. D **12**, 2060 (1976)
25. A.I. Signal, A.W. Thomas, Phys. Lett. B **211**, 481 (1988); Phys. Rev. D **40**, 2832 (1989)

26. A.W. Schreiber, A.W. Thomas, J.T. Londergan, Phys. Rev. D **42**, 2226 (1990)
27. A.W. Schreiber, A.I. Signal, A.W. Thomas, Phys. Rev. D **44**, 2653 (1991)
28. P.J. Sutton, A.D. Martin, R.G. Roberts, W.J. Stirling, Phys. Rev. D **45**, 2349 (1992)
29. M. Glück, E. Reya, I. Schienbein, Eur. Phys. J. C **10**, 313 (1999)
30. M. Glück, E. Reya, A. Vogt, Z. Phys. C **53**, 651 (1992)
31. R.G. Roberts, The structure of the proton (Cambridge University Press, 1990)
32. R.D. Field, R.P. Feynman, Phys. Rev. D **15**, 2590 (1977)
33. G.V. Dunne, A.W. Thomas, K. Tsushima, hep-ph/0107042
34. M. Glück, E. Reya, Mod. Phys. Lett. A **15**, 883 (2000); M. Glück, E. Reya, M. Stratmann, W. Vogelsang, hep-ph/0011215